Published OnlineFirst August 15, 2013; DOI: 10.1158/0008-5472.CAN-13-0344

Cancer Research

Cetuximab Attenuates Its Cytotoxic and Radiosensitizing Potential by Inducing Fibronectin Biosynthesis

Iris Eke[1,2], Katja Storch[1], Mechthild Krause[1,2,3,4], and Nils Cordes[1,2,5]

Abstract

Inherent and acquired resistance to targeted therapeutics continues to emerge as a major clinical obstacle. For example, resistance to EGF receptor targeting occurs commonly, more so than was expected, on the basis of preclinical work. Given emerging evidence that cancer cell–substrate interactions are important determinants of therapeutic sensitivity, we examined the impact of cell–fibronectin interactions on the efficacy of the EGF receptor antibody cetuximab, which is used widely for lung cancer treatment. Our results revealed the potential for cell–fibronectin interactions to induce radioresistance of human non–small cell lung cancer cells. Cell adhesion to fibronectin enhanced tumor cell radioresistance and attenuated the cytotoxic and radiosensitizing effects of cetuximab. Both *in vitro* and *in vivo*, we found that cetuximab treatment led to a remarkable induction of fibronectin biosynthesis. Mechanistic analyses revealed the induction was mediated by a p38–MAPK–ATF2 signaling pathway and that RNAi-mediated inhibition of fibronectin could elevate the cytotoxic and radiosensitizing potential of cetuximab. Taken together, our findings show how cell adhesion blunts cetuximab, which, by inducing fibronectin, generates a self-attenuating mechanism of drug resistance. *Cancer Res; 73(19); 1–11. ©2013 AACR.*

Introduction

Molecular therapies have opened a promising novel approach to overcome tumor–type-dependent cancer cell resistance to radio- and chemotherapy (1, 2). Overexpressed in lung, head and neck, colorectal, and breast carcinomas as well as glioblastomas and other tumors, the EGF receptor (EGFR) serves as targetable key promoter of tumor growth and progression (3). Inhibitory components block either the cytoplasmic EGFR tyrosine kinase or the extracellular ligand-binding domain to suppress prosurvival and mitogenic downstream signaling (4). However, clinical evaluations of these targeting strategies showed differential efficacy mostly falling below expectations from preclinical analysis (5, 6).

In a phase III clinical trial on head and neck squamous cell carcinomas (HNSCC), cetuximab significantly increased locoregional tumor control and overall patient survival in combination with radiotherapy as compared with radiotherapy alone (7, 8) whereas studies in colorectal cancers using cetuximab monotherapy indicated a small benefit in the time to disease progression (9). Only recently, in phase II and III clinical trials, was the feasibility of combined cetuximab administration given simultaneously to standard platinum-based chemotherapeutics or radiochemotherapy shown, resulting in improved survival of patients with non–small cell lung cancer (NSCLC; ref. 10). For individualized patient identification and triage for cetuximab therapy, an intensive search for resistance factors is ongoing as three potential indicators, that is, EGFR copy number (11), nuclear EGFR localization, and KRAS mutational status (12–14), have failed to predict cetuximab efficacy in NSCLC. Therefore, the molecular mechanisms attenuating cetuximab's efficacy remain to be determined.

Integrin-mediated adhesion to extracellular matrix (ECM) might play an essential role in reducing cetuximab activity as a result of cooperative reciprocal actions and transactivation between EGFR and integrin cell adhesion receptors. This could occur through Src-dependent p130Cas phosphorylation (15), phosphatidylinositide 3 kinase (PI3K)/Akt (16), and JNK-interacting protein-4/JNK2 signaling (17); integrin-mediated adhesion to ECM might play an essential role in reducing cetuximab activity. Previous work showed attenuated cytotoxicity and radiosensitization of EGFR tyrosine kinase inhibitors like BIBX1382BS or Iressa by cell adhesion to ECM (18–20). Taking the role of ECM in determining EGFR transcriptional responses, EGFR–integrin transactivation and integrin-mediated ECM protein synthesis into consideration (21, 22), we hypothesize that EGFR signaling critically contributes to the regulation of ECM protein synthesis and secretion, which, in turn, could modulate radio-, chemo-, and cetuximab resistance.

Authors' Affiliations: [1]OncoRay—National Center for Radiation Research in Oncology; [2]Department of Radiation Oncology, Medical Faculty Carl Gustav Carus, Technische Universität Dresden; [3]German Cancer Consortium (DKTK); [4]German Cancer Research Center (DKFZ); and [5]Institute of Radiooncology, Helmholtz Center Dresden–Rossendorf, Dresden, Germany

Note: Supplementary data for this article are available at Cancer Research Online (http://cancerres.aacrjournals.org/).

Corresponding Author: Nils Cordes, OncoRay—National Center for Radiation Research in Oncology, Medical Faculty Carl Gustav Carus, Dresden University of Technology, Fetscherstrasse 74/PF 41, 01307 Dresden, Germany. Phone: 490-351-458-7401; Fax: 490-351-458-7311; E-mail: nils.cordes@oncoray.de

doi: 10.1158/0008-5472.CAN-13-0344

Published OnlineFirst August 15, 2013; DOI: 10.1158/0008-5472.CAN-13-0344

Fibronectin is abundantly expressed in various human tumors (23), and it has been postulated to aid in the promotion of tumor growth and progression as a result of participating in the development of an ideal microenvironment through extensive ECM remodeling (24–27). Transcription of the *FN* gene is accomplished by p38 mitogen-activated protein kinase (MAPK) activation and cyclic AMP response element (CRE)/CCAAT site-dependent phosphorylation of the activating transcription factor 2 (ATF2; refs. 28, 29). Additional transcription factors involved in *FN* gene transcription are CRE-binding protein (CREB) and early growth response-1 (EGR-1; refs. 30, 31). Participation of the EGFR in ECM protein biosynthesis has not been documented to date. Therefore, we investigated the possibility that reduction or loss of cetuximab-mediated cytotoxicity and radiosensitization of NSCLC cells arises from cell adhesion to fibronectin as well as from and effect of cetuximab itself on extensive stimulation of fibronectin biosynthesis and secretion. We show that cetuximab-induced cytotoxicity and radiosensitization is reduced when cells are adherent to fibronectin. Mechanistically, application of cetuximab promotes fibronectin biosynthesis and secretion via p38 MAPK/ATF2 signaling. This study indicates a critical role for ECM proteins in cetuximab resistance in human NSCLC.

Materials and Methods

Antibodies and reagents

Antibodies against fibronectin, 5-bromo-2-deoxyuridine (BrdU; BD), phospho-EGFR Tyrosine(Y)1173, phospho-EGFR Y1068, phospho-EGFR Y845 (Biosource), phospho-Akt Serine (S)473, phospho-Akt Threonine(T)308, Akt, phospho-ERK1/2 T202/Y204, ERK1/2, phospho-p38 MAPK T180/Y182, p38 MAPK, phospho-JNK T183/Y185, JNK, phospho-MEK1/2 S217/221, MEK1/2, phospho-ATF2 T69/71, ATF2, phospho-CREB S133, CREB, EGR1 (Cell Signaling Technology), β-actin (Sigma), horseradish peroxidase-conjugated donkey anti-rabbit and sheep anti-mouse (Amersham), Alexa594 anti-mouse and Alexa488 anti-rabbit (Invitrogen) were purchased as indicated. Enhanced chemiluminescent reagent (ECL) was from Amersham, Oligofectamine and Lipofectamine 2000 from Invitrogen, BrdU and BSA from Serva, RNase A type III-A from Sigma, and pepsin 0.7 FIP-U from Merck. Vectashield/4′, 6-diamidino-2-phenylindole (DAPI) mounting medium was from Alexis, and Alexa Flour 594 Phalloidin from Molecular Probes.

Cell culture and radiation exposure

A549 and H1299 cells were purchased from the American Tissue Culture Collection in 2006. Since then, cells were passaged less than 30 times before experiments were conducted. Cells were cultured in Dulbecco's Modified Eagle Medium (DMEM) containing GlutaMax-I supplemented with 10% fetal calf serum (FCS; PAA) and 1% non-essential amino acids (PAA) at 37°C in a humidified atmosphere containing 10% CO_2 (pH 7.4). Where indicated, cells were grown on fibronectin (1 μg/cm^2; BD) precoated plates as previously published (18). In all experiments, asynchronously growing cells were used. Irradiation was delivered at room temperature using single doses of 200 kV X-rays (~1.3 Gy/min, 20 mA; Yxlon Y.TU 320; Yxlon) filtered with 0.5 mm Cu. In fractionation experiments, single doses of 2 Gy/d were delivered on three consecutive days. The absorbed dose was measured using a Duplex dosimeter (PTW).

Colony formation assay

The colony formation assay was applied for measurement of clonogenic cell survival as previously described (32). In brief, cells were grown on fibronectin or without substrate (poly-S) for 24 hours. Before irradiation, cells were incubated with cetuximab (0–20 μg/mL; Merck). After 8 days, cells were stained with Coomassie blue and cell colonies (>50 cells) were counted. Plating efficiencies were calculated as follows: numbers of colonies formed/numbers of cells plated. Surviving fractions were calculated as follows: numbers of colonies formed/(numbers of cells plated (irradiated) × plating efficiency (unirradiated)). Each point on survival curves represents the mean surviving fraction from at least three independent experiments.

Real-time PCR

Cells were plated on poly-S ± FCS and treated with cetuximab (5 μg/mL). After 24 and 48 hours, cells were isolated and total RNA was extracted using the NucleoSpin RNA II kit (Macherey-Nagel) according to the manufacturer's instructions. Then, RNA was transcribed into cDNA (Superscript III Reverse Transcriptase, Invitrogen). Reactions were conducted using the LightCycler FastStart DNA Master PLUS HybProbe kit (Roche) and specific primers and probes (TIB MOLBIOL; Supplementary Table S2). The expression level of fibronectin was normalized to the expression of the housekeeping gene TATA-box binding protein.

Total protein extracts and Western blot

Cells grown either on poly-S or fibronectin ± FCS were treated with cetuximab (5 μg/mL). Where indicated, cells were incubated with EGF (20 ng/mL; Calbiochem) for 15 minutes. For lysis, cells were rinsed with ice-cold PBS before adding modified radioimmunoprecipitation assay (RIPA) buffer (50 mmol/L Tris–HCl; pH 7.4, 1% Nonidet-P40, 0.25% sodium deoxycholate, 150 mmol/L NaCl, 1 mmol/L EDTA, Complete protease inhibitor cocktail (Roche), 1 mmol/L $NaVO_4$, 2 mmol/L NaF), scraping and measuring total protein amounts with the BCA assay (Pierce). After SDS–PAGE and transfer of proteins onto nitrocellulose membranes (Schleicher and Schuell), probing and detection of specific proteins was accomplished with indicated antibodies and ECL as described previously (18). Dot blotting was employed for determining secreted matrix proteins upon C225 (5 μg/mL) exposure. The medium was dropped onto nitrocellulose membranes and matrix proteins were detected with indicated antibodies and ECL.

Immunofluorescence staining

Localization of ATF2 and CREB was analyzed in cells grown on poly-S with or without 48-hour cetuximab treatment (5 μg/mL). Staining of proteins was accomplished with specific antibodies, Alexa Fluor 594 Phalloidin, and Vectashield/DAPI mounting medium. Alexa Fluor 568-labeling of cetuximab by Protein Labeling Kit (Invitrogen) was employed for EGFR

Published OnlineFirst August 15, 2013; DOI: 10.1158/0008-5472.CAN-13-0344

localization studies of 1% formaldehyde/PBS fixed and 0.25% Triton X-100/PBS permeabilized cells.

Tumor xenograft models and combined treatment with cetuximab plus fractionated irradiation

To assess the effects of cetuximab *in vivo*, A549 tumor xenografts were investigated. Animal facilities and experiments were approved by the Landesdirektion Dresden (Dresden, Germany), according to the German animal welfare regulations. Immunocompromised 7- to 14-week-old male and female NMRI (nu/nu) mice (Experimental Centre of the Medical Faculty Carl Gustav Carus; Technische Universität Dresden) were further immunosuppressed by whole-body irradiation. Tumor pieces were transplanted on the hindleg of anesthetized nude mice as described previously (32, 33). At a diameter of approximately 7 mm, animals were treated with two injections of cetuximab (1 mg/injection per mouse) intraperitoneally at day 0 and 7. Six hours after the second injection, cetuximab-treated and control tumors were excised, cut into halves, and either snap-frozen in liquid nitrogen or fixed in formalin and embedded in paraffin as described previously (32, 33). Then, immunohistochemistry was conducted on paraffin-embedded tumors using the Vectastain Elite ABC Kit (Vector Laboratories) and anti-Fibronectin antibody (BD). For tumor growth-delay experiments, A549 tumor pieces were taken from a cryoconserved source and transplanted subcutaneously into the hind leg of anesthetized and whole–body-irradiated nude mice. After reaching a tumor diameter of 6 mm ($\sim$100 mm^3), treatment schedules were started. The animals received either cetuximab alone (1 injection day 0; 1 mg cetuximab per animal per injection) plus 30 irradiation fractions in six weeks to graded total doses. Tumor growth time (time to reach 5-fold the starting volume) was evaluated as described previously (34).

siRNA-mediated knockdown of EGFR, ITGB1, ITGA5, fibronectin, p38 MAPK, and ATF2

Fibronectin siRNA (sense: 5′-GGACAUCCUAUAGAAUUGGtt-3′), EGFR siRNA (sense: 5′-GGCACGAGUAACAAGCUCAtt-3′), ITGB1 siRNA (sense: 5′-GGAACCCUUGCACAAGUGAtt-3′), ITGA5 siRNA (sense: 5′-GGGAACCUCACUUACGGCUtt-3′), MEK1 siRNA (sense: 5′-GGAGCUAGAGCUUGAUGAGtt-3′), p38 MAPK siRNA (sense: 5′-GGAAUUCAAUGAUGUGUAUtt-3′) and ATF2 siRNA (sense: 5′-CCAGGAUAGUCCUUUACCUtt-3′), were obtained from Applied Biosystems. A nonspecific siRNA (sense: 5′-GCAGCUAUAUGAAUGUUGUtt-3′; MWG) was used as control. Cells were prepared for siRNA transfection (20 nmol/L) with oligofectamine under serum-free conditions as previously described (35). Twenty-four hours after transfection, cells were trypsinized and subjected to colony formation, real-time PCR, or Western blot.

Kinase assays

Cells were incubated with cetuximab (5 μg/mL) for one hour or Ly294002 (20 μmol/L), PD98059 (25 μmol/L), SP600125 (10 μmol/L), or SB203680 (20 μmol/L) for 30 minutes. Kinase activity of Akt, ERK1/2, JNK, and p38 MAPK was measured according to the manufacturer's protocol and as recently published (33).

Cell-cycle analysis

Cell-cycle measurements have been conducted as described previously (19) and as described in Supplementary Materials.

Promotor assay

Deletion mutants of the human *FN*1 promoter were amplified from DNA isolated from human blood with the QIAamp Blood Kit (Qiagen) with specific primers according to *FN*1 5′-untranslated region and 5′ flanking genomic sequences (NCBI Reference Sequence No. NT_005403.17). Sequences amplified encompassed nucleotides −530/+266 and −171/+266 of the human *FN*1 promoter with flanking Kpn I/Xho I restriction sites (specific primers -530fw: 5′-gg-ggtacc-GGATTCTTAACAGCTGCAAGG-3′; -171fw: 5′-gg-ggtacc-GAGCCCGGGCCAATCGGCG-3′; +266rev: 5′-ccg-ctcgag-GTTGAGACGGTGGGGGAGAG-3′). PCR products were inserted into Kpn I/Xho I sites of pGL3 Basic luciferase reporter plasmid (Promega). For luciferase reporter gene expression under the control of the different promoter constructs, cells were transiently transfected with pGL3 constructs and pRL-TK *Renilla* luciferase expression vector (Promega) as internal control of transfection efficiency. Cells were examined after EGFR knockdown (nonspecific siRNA was used as control). pCMV control vector was used as positive control, whereas the pGL3 Basic vector without promoter was transfected as negative control. Measurement of luciferase expression was done with the Dual-Luciferase Reporter Assay System (Promega) according to the manufacturer's protocol. Promotor activity was calculated as follows: (luciferase activity *FN*1 promotor/*Renilla*) − (luciferase activity pGL3 Basic/*Renilla*). Results were normalized to −530/+266 *FN*1 promotor activity in control siRNA cells.

Microarray datasets

For analysis of *FN1* (Fibronectin) mRNA expression, Oncomine transcriptom datasets were searched for studies comparing patients with NSCLC at different tumor stages (I–IV) or different overall survival time (alive after three years vs. dead after three years; Supplementary Table S1). The normalized values of the individual datasets were combined and further analyzed with regard to differential gene expression using the 2-sided Student *t* test.

Data analysis

Means ± SD of at least three independent experiments were calculated with reference to untreated controls defined in a 1.0 scale. To test statistical significance, Student *t* test was conducted using Microsoft Excel 2003. Results were considered statistically significant if a *P* value of less than 0.05 was reached.

Results

Fibronectin expression is increased in advanced NSCLC and adhesion to ECM potently attenuates cetuximab-mediated cytotoxicity and radiosensitization

According to a DNA microarray database search (www.oncomine.org), fibronectin expression in NSCLC significantly ($P < 0.01$) increases with higher Union Internationale Contre le Cancer (UICC) stage as compared with limited disease NSCLC (stage I; Fig. 1A; $n = 421$). In addition, the tumor fibronectin

Published OnlineFirst August 15, 2013; DOI: 10.1158/0008-5472.CAN-13-0344

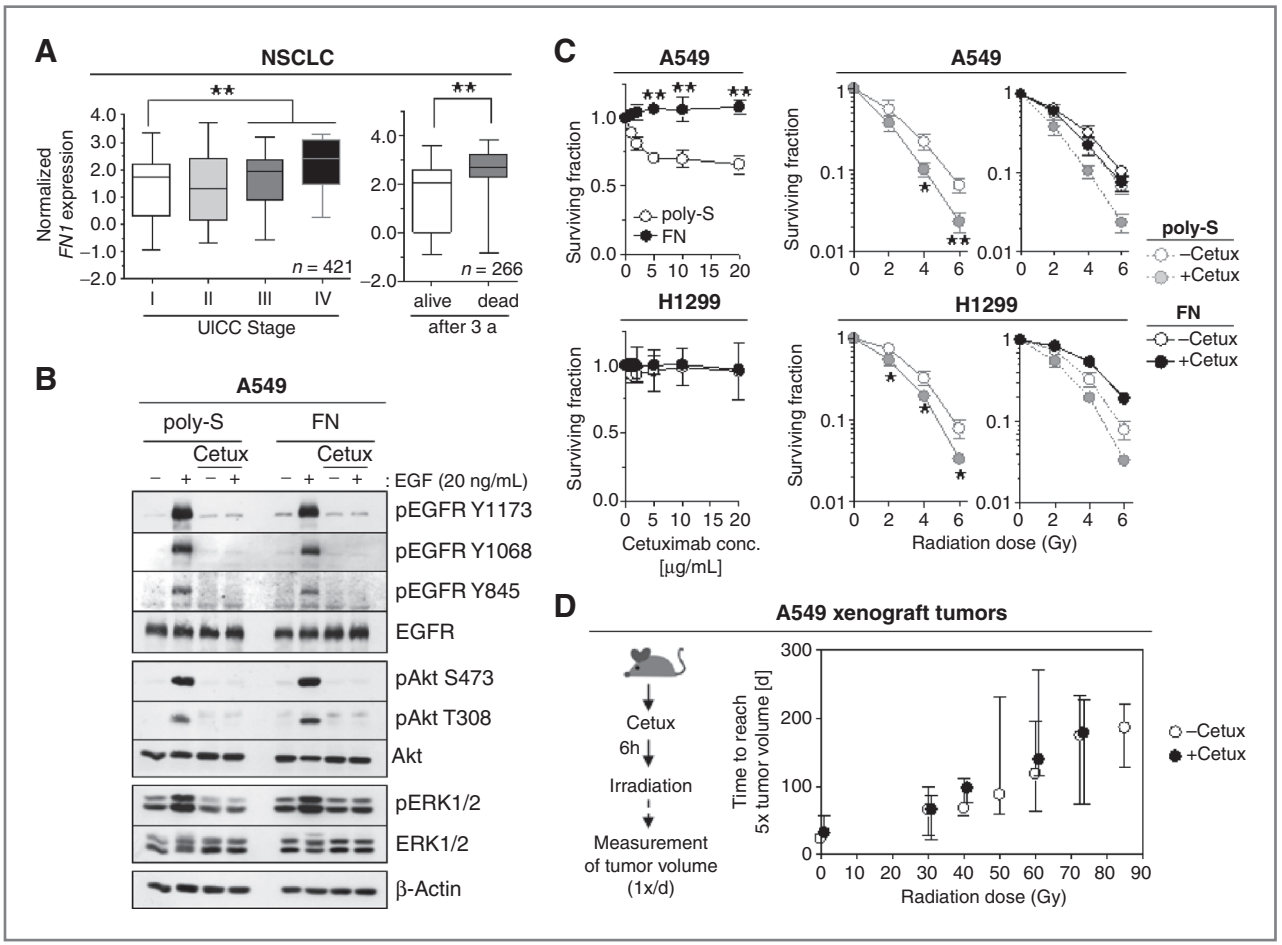

Figure 1. Adhesion to fibronectin abrogates the cytotoxic and radiosensitizing potential of cetuximab in human NSCLC cells. A, *Fibronectin 1* (*FN1*) mRNA expression analysis (Oncomine) in NSCLC biopsies according to different UICC stages or 3-year overall patient survival (studies are shown in Supplementary Table S1). B, Western blot analysis of total and phosphorylated EGFR and downstream proteins in cells plated on cell culture plastic (poly-S) or fibronectin. Twenty-four hour serum starvation was followed by treatment of cells with cetuximab (5 μg/mL, one hour) and/or EGF (20 ng/mL, 5 minutes) where indicated. β-Actin served as loading control. C, clonogenic survival and clonogenic radiation survival of poly-S or fibronectin NSCLC cell cultures treated with different concentrations of cetuximab (0–20 μg/mL) or with cetuximab (5 μg/mL) for 24 hours followed by irradiation. Data show mean ± SD. ($n = 3$; *, $P < 0.05$; **, $P < 0.01$; *t* test). D, experimental *in vivo* setup. A549 xenografts were grown to a diameter of 6 mm. Subsequently, mice received cetuximab (1 mg/kg) or 1 × PBS (control) injections. X-ray irradiation was applied 6 hour after second antibody/1 × PBS injection. Time to reach 5-fold tumor starting volume upon cetuximab treatment is plotted against radiation dose (medians ± 95% CI; $n = 10$–18).

expression in patients who died within 3 years after biopsy, was also significantly ($P < 0.01$) higher than in patients who were still alive after 3 years (Fig. 1A; $n = 266$). Based on the ability of cetuximab to efficiently inhibit EGFR in a substratum-independent manner (Fig. 1B and Supplementary Fig. S1A and 1B), we treated A549 and H1299 cells with cetuximab alone or in combination with single or fractionated doses of X-rays. Intriguingly, the cetuximab-dependent cytotoxicity and radiosensitization observed on polystyrene (poly-S) was strongly diminished when cells grew on fibronectin (Fig. 1C and Supplementary Fig. S1C). These effects were detectable both after single and fractionated irradiation (Fig. 1C and Supplementary Fig. S1C). Proliferation kinetics and cell-cycling data generated under similar experimental conditions showed that these findings were not due to cell-cycle effects of cetuximab or fibronectin (Supplementary Fig. S1D and S1E). Notably, H1299 cells were resistant to cetuximab monotherapy but showed radiosensitization when grown on poly-S (Fig. 1C). Moreover, radiation survival was significantly ($P < 0.01$) higher in ECM-grown cultures than in poly-S cultures, which illustrates the prosurvival effects of ECM adhesion (Fig. 1C). To test for the efficacy of cetuximab *in vivo*, A549 xenografts tumors were treated with varying single doses of X-rays without and in combination with cetuximab for tumor volume and control probability (Fig. 1D). Despite a slight and nonsignificant delay in tumor growth by cetuximab alone, cetuximab did not significantly affect growth of irradiated A549 tumors as shown for the time to reach the 5-fold tumor volume (Fig. 1D). Thus, cell adhesion to fibronectin and *in vivo* growth conditions effectively attenuate cetuximab antisurvival effects in NSCLC cells and tumors in nude mice.

Published OnlineFirst August 15, 2013; DOI: 10.1158/0008-5472.CAN-13-0344

Integrins mediate the effect of fibronectin on cetuximab efficacy

On the basis of these observations, we next assessed how extracellular fibronectin impacts on survival and radiosensitization upon EGFR inhibition. As the heterodimeric α5β1 integrin receptor is the main mediator for binding of cells to fibronectin, we carried out a combined knockdown of these two integrin subunits and monitored changes in basal and radiation survival of cetuximab-treated fibronectin cell cultures. Efficient α5β1 integrin depletion (Fig. 2A) resulted in unmodified basal cell survival (Fig. 2A). Interestingly, α5β1 integrin-depleted fibronectin cell cultures were sensitized to cetuximab monotherapy (Fig. 2A) as compared to controls (Fig. 1C). Based on radiosensitization mediated by downregulation of α5β1 integrin (Fig. 2A), these data suggest that the α5β1 integrins are critical in the process of cetuximab attenuation observed in fibronectin-adherent NSCLC cells.

Cetuximab enhances fibronectin biosynthesis

Subsequently, we analyzed whether EGFR and cetuximab are involved in fibronectin biosynthesis. Twenty-four and 48-hour serum-starvation-control experiments (to evaluate the effects of growth factor withdrawal) revealed a significant elevation in *FN* mRNA and protein synthesis (Supplementary Fig. S2A–E). Cetuximab induced *FN* mRNA in A549 cells and protein expression in A549 and H1299 cells *in vitro* (Fig. 2B and C) and *in vivo* in A549 tumor xenografts (Fig. 2E). To prove EGFR dependence of these results, we depleted EGFR expression by siRNA and found a significant ($P < 0.01$) increase of

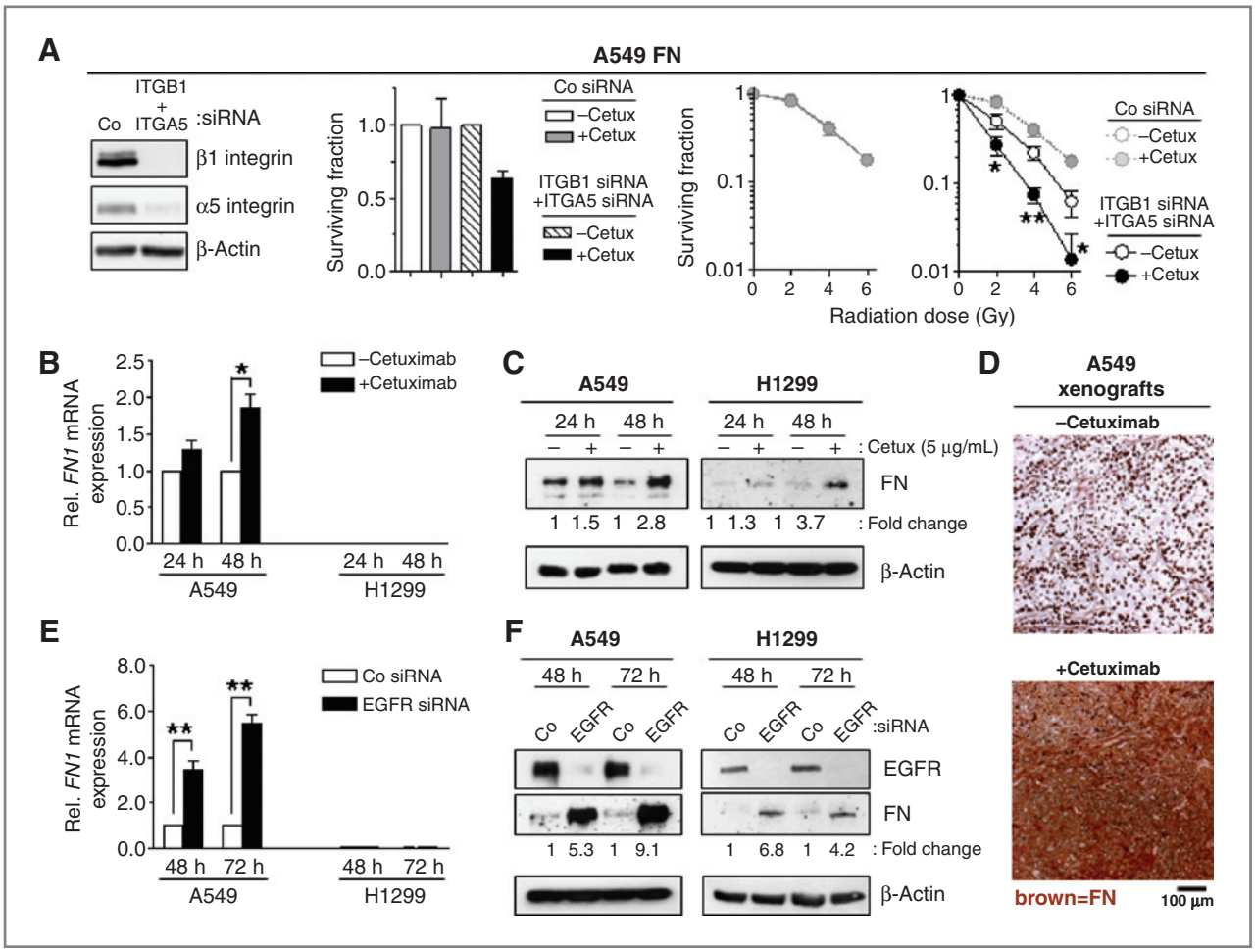

Figure 2. EGFR inhibition stimulates fibronectin biosynthesis *in vitro* and *in vivo*. A, Western blot, clonogenic survival, and radiation survival of A549 cells after siRNA-mediated knockdown of β1 integrin (ITGB1) and α5 integrin (ITGA5). Cells were cultured on fibronectin and treated with cetuximab (Cetux, 5 μg/mL) for 24 hours before irradiation. Nonspecific siRNA was used as control. B, *FN1* mRNA expression of NSCLC cells treated with cetuximab (5 μg/mL) for 24 or 48 hours, measured by real-time PCR. The TATA-box binding protein was used as housekeeping gene. Samples were normalized to untreated A549 cultures ($n = 2$; *, $P < 0.05$; *t* test). B, Western blot analysis of fibronectin in NSCLC cells lyzed after a 24 or 48 hours treatment with cetuximab (5 μg/mL). β-Actin served as loading control. C, confocal fluorescence images of fibronectin expression (green) in 24-hour cetuximab-treated NSCLC cells (5 μg/mL). Nuclei were stained with DAPI. D, immunohistochemistry for fibronectin in untreated or cetuximab-treated A549 tumor xenografts. Representative images are shown. E, at 24 or 48 hours after siRNA knockdown of EGFR (Co, nonspecific control siRNA), real-time PCR analysis of fibronectin was conducted and normalized to A549 controls (mean ± SD; $n = 3$; **, $P < 0.01$; *t* test). F, EGFR and fibronectin expression in EGFR knockdown cell cultures were analyzed by Western blotting. β-Actin served as loading control.

Published OnlineFirst August 15, 2013; DOI: 10.1158/0008-5472.CAN-13-0344

fibronectin levels 48 and 72 hours after knockdown relative to controls (Fig. 2E and F and Supplementary Fig. S2D).

Fibronectin depletion promotes the cytotoxic and radiosensitizing potential of cetuximab

To provide evidence that fibronectin is a key antagonist of cetuximab efficacy, fibronectin secretion by NSCLC cells was impaired by siRNA-mediated silencing of fibronectin expression, and these cells were treated with cetuximab (Fig. 3A). The data revealed an increase in cetuximab cytotoxicity under absent or very low fibronectin levels (Fig. 3B and C). Similarly, fibronectin depletion rendered A549 and H1299 cells significantly ($P < 0.01$) more radiosensitive relative to controls (Fig. 3D).

EGFR remains localized to the cell membrane and p38 MAPK, and JNK1 phosphorylation is induced on cetuximab treatment

The subcellular cetuximab–EGFR interaction and the responsible signaling molecules involved in cetuximab-mediated fibronectin induction were evaluated next. Immunofluorescence EGFR staining in combination with Alexa Fluor 568-labeled cetuximab of A549 and H1299 cells and cetuximab-treated EGFR-CFP A549 transfectants revealed stable membranous EGFR localization throughout the examined 48-hour time period (Fig. 4A and Supplementary Fig. S3). Concomitantly, EGFR-Y1173 and Akt-S473 phosphorylation remained unchanged whereas EGFR-Y1068 showed a transient, monophasic dephosphorylation, in contrast to stable hypophosphorylation of ERK1/2-T202/Y204 representing the only protein kinase altered in a selective phosphoprotein array (Fig. 4B–D). Intriguingly, JNK1-T183/Y185 and p38 MAPK-T180/Y182, which were not represented in the array, exhibited a hyperphosphorylation upon cetuximab exposure (Fig. 4C and D).

p38 MAPK plays an essential role in cetuximab-dependent fibronectin production

Next, we sought to analyze the activities of EGFR-associated protein kinases potentially inducing fibronectin expression via cetuximab. In line with protein phosphorylations shown in Fig. 4, cetuximab resulted in unaltered Akt, reduced ERK1/2, and increased JNK and p38 MAPK kinase activities (Fig. 5A and B). Inhibitors for PI3K (Ly294002), MAPK (PD59009), MEK1 (U0126), and the p38 MAPK inhibitor (SB203680) potently attenuated or reduced the corresponding protein kinase activity (Fig 5A) or phosphorylation (Fig. 5B). However, cetuximab-induced fibronectin expression was exceptionally diminished by p38 MAPK inhibition using SB203680 (Fig. 5B) – a finding confirmed by p38 MAPK siRNA knockdown (Fig. 5C). These data also strongly suggest a particular involvement of EGFR-MEK1/2-ERK1/2 signaling in fibronectin biosynthesis, as inhibition of MEK1/2 showed similar fibronectin induction (Fig. 5B and Supplementary Fig. S4) as observed with EGFR inhibition (see Fig. 2).

Cetuximab-induced fibronectin expression is ATF2 dependent

The transcription factor that controls fibronectin biosynthesis downstream of cetuximab-inhibited EGFR was evaluated next. ATF2, a known transcription factor for the *FN1* gene,

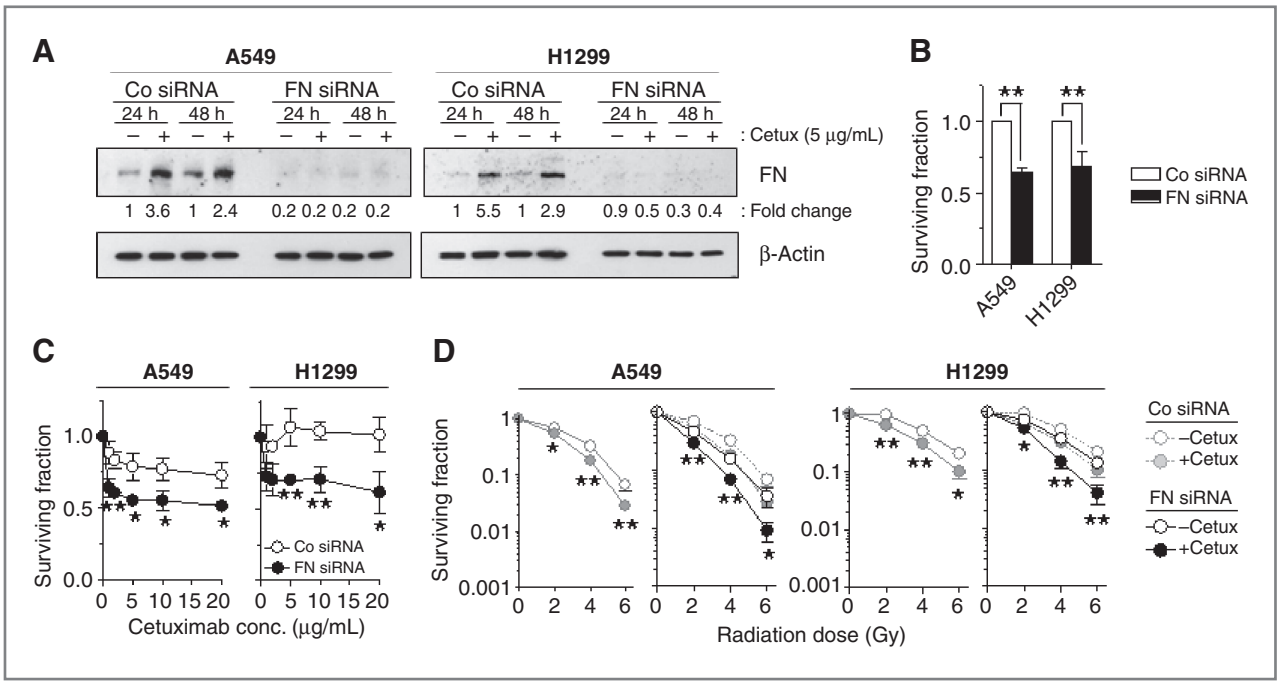

Figure 3. Inhibition of cetuximab-induced fibronectin upregulation increases the efficacy of cetuximab. A, Western blot of fibronectin knockdown cultures treated with cetuximab (Cetux, 5 μg/mL) for 24 or 48 hours. B, colony formation of NSCLC cells after fibronectin siRNA transfection relative to nonspecific siRNA controls (Co). Data show mean ± SD ($n = 3$; **, $P < 0.01$; t test). C and D, survival (C) and radiation survival (D) of fibronectin knockdown cultures. Treatment with cetuximab was carried out 24 hours before irradiation. Data are shown as means ± SD ($n = 3$; *, $P < 0.05$; **, $P < 0.01$; t test).

Published OnlineFirst August 15, 2013; DOI: 10.1158/0008-5472.CAN-13-0344

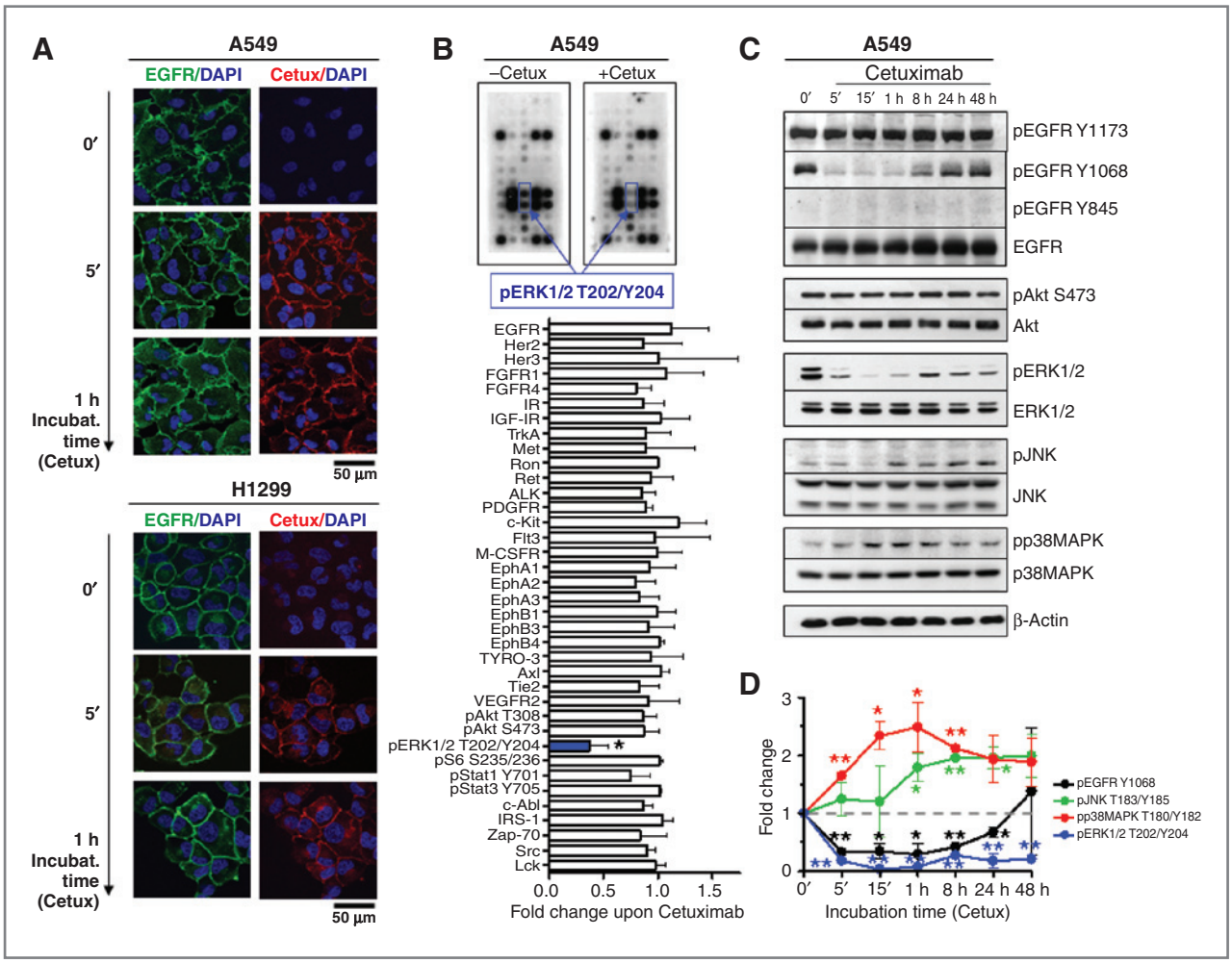

Figure 4. Treatment with cetuximab leads to enhanced p38 MAPK and JNK phosphorylation. A, confocal fluorescence images on the subcellular localization of EGFR (green) at different time points after treatment with Alexa Fluor 568-labeled cetuximab (red). Nuclei were stained with DAPI. B, A549 cells were treated with cetuximab (5 μg/mL). After one hour, the RTK signaling array was conducted as described under Material and Methods. Data are shown as fold-change relative to untreated cells (means ± SD; $n = 2$; *, $P < 0.05$; *t* test). C and D, Western blot (C) and densitometric (D) analysis (means ± SD; $n = 3$; *, $P < 0.05$; **, $P < 0.01$; *t* test) of A549 cells treated with cetuximab (5 μg/mL). Cells were lysed at indicated time points. β-Actin was used as loading control.

exhibited T69/71 hyperphosphorylation on cetuximab treatment or EGFR depletion in A549 and H1299 cells whereas other putative transcription factors for the *FN1* gene promoter, that is, CREB and EGR1, remained unaltered (Fig. 6A and B and Supplementary Fig. S5). This ATF2 hyperphosphorylation mainly occurred in the cell nucleus after cetuximab treatment visualized by immunofluorescence staining (Fig. 6C). Using ATF2 knockdown, fibronectin biosynthesis by cetuximab was maintained at basal levels, indicating a critical function of ATF2 in this context (Fig. 6D). We further provide evidence for p38 MAPK signaling to ATF2 for fibronectin biosynthesis regulation indicated by absent ATF2 hyperphosphorylation on cetuximab treatment under siRNA-mediated knockdown or pharmacologic inhibition of p38 MAPK (Fig. 6E and F). Finally, it is shown that deletion of the −530 to −171 bp sequence of *FN1* gene promoter region, which include the ATF2 binding sites, prevented the induction of *FN1* promoter activity after EGFR inhibition (Fig. 6G and Supplementary Fig. S6). Based on unchanged CREB phosphorylation and subcellular localization on cetuximab treatment, we exclude an essential role of this transcription factor in the investigated context. From these observations, we hypothesize a direct function of ATF2 in *FN1* gene transcription and fibronectin protein synthesis on cetuximab-mediated EGFR inhibition (Fig. 6H).

Discussion

Resistance mechanisms against modern molecular drugs are, with specific exceptions, not well understood. Due to its prominent role in cancer cell proliferation, EGFR has been targeted with antibodies or pharmacologic inhibitors with the intention to reduce tumor growth and enhance sensitization to conventional radio(chemo)therapy. Regarding these goals, the additional administration of anti-EGFR compounds to radio(chemo) therapeutic regimes has resulted in a range of responses in different EGFR-overexpressing tumor types. In general, anti-EGFR therapies have failed to meet the outcome predicted by

Published OnlineFirst August 15, 2013; DOI: 10.1158/0008-5472.CAN-13-0344

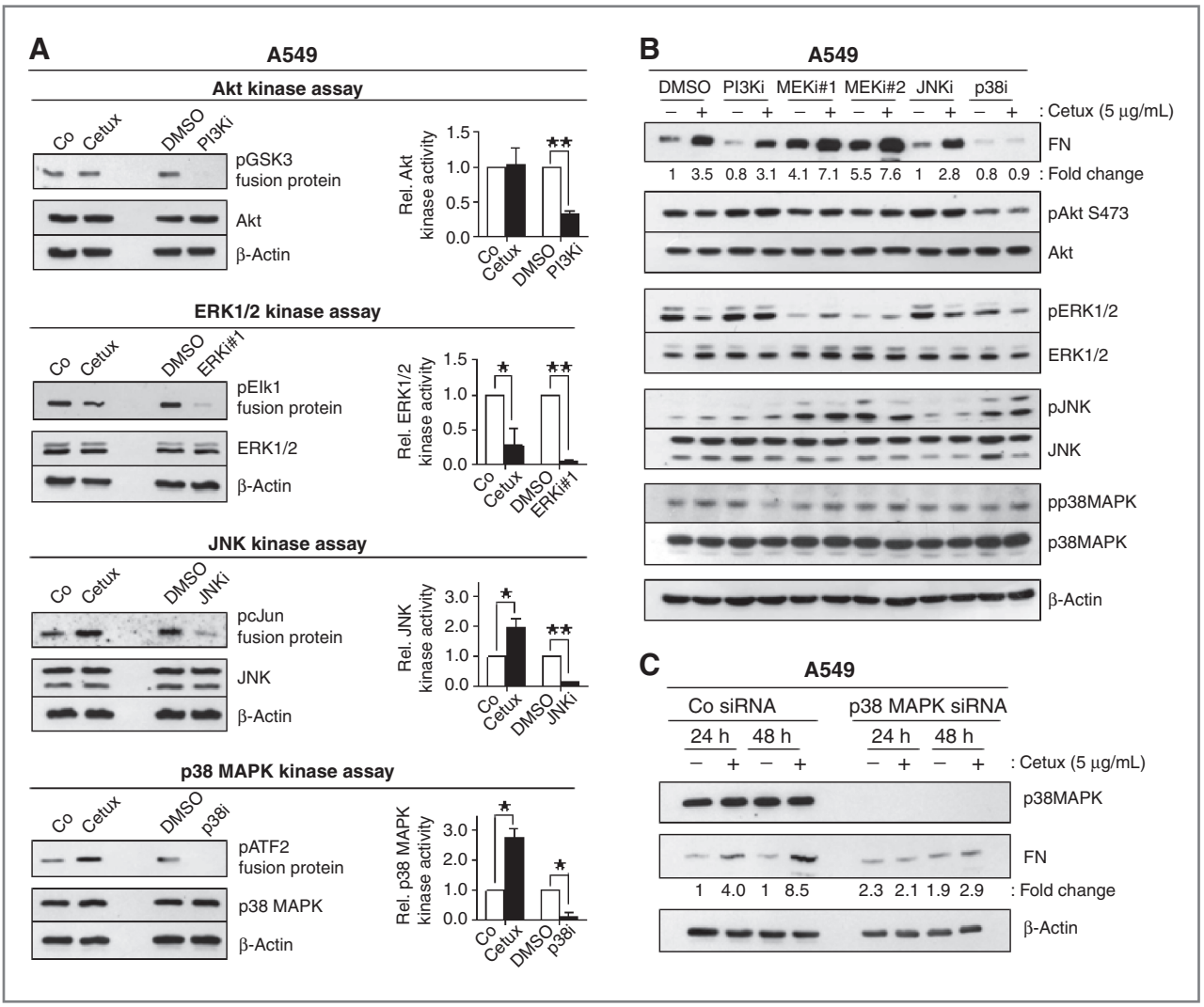

Figure 5. Inhibition of p38 MAPK impairs cetuximab-induced fibronectin synthesis. A, Western blot analysis of kinase assays and input lysates from A549 cells treated with cetuximab (5 μg/mL) for one hour or with PI3Ki (Ly294002, 20 μmol/L), MEKi (PD98059, 25 μmol/L), JNKi (SP600125, 10 μmol/L), or p38i (SB203680, 20 μmol/L) for 30 minutes. Fold changes were calculated from densitometric analysis of protein bands of phosphorylated fusion proteins (mean ± SD; $n = 2$; *, $P < 0.05$; **, $P < 0.01$; t test). B, A549 cells were treated with PI3Ki (Ly294002, 20 μmol/L), MEKi#1 (PD98059, 25 μmol/L), MEKi#2 (U0126, 10 μmol/L), JNKi (SP600125, 10 μmol/L), or p38i (SB203680, 20 μmol/L) 30 minutes before cetuximab (5 μg/mL). After 48 hours, cells were lysed and expression and phosphorylation of indicated proteins were analyzed by Western blot. C, after siRNA-mediated knockdown of p38 MAPK, A549 cells were treated with cetuximab for 24 or 48 hours. Nonspecific siRNA (Co) was used as control.

preclinical investigations. Definite criteria for patient selection are missing. In addition, intra- and/or extracellular resistance mechanisms can be induced by drugs such as cetuximab raising questions as to the rationale and benefits for their clinical use in unselected patients. Here, we identified a novel resistance mechanism by showing that fibronectin biosynthesis is pronouncedly stimulated by cetuximab-mediated EGFR inhibition in human NSCLC cells and NSCLC tumor xenografts. Although adhesion to fibronectin attenuated cetuximab's cytotoxic and radiosensitizing efficacy, depletion of fibronectin sensitized NSCLC cells to cetuximab through a mechanism specifically involving p38 MAPK-ATF2 signaling.

ECM protein expression patterns are tremendously changed during carcinogenesis and tumorigenesis as a result of excessive ECM remodeling by destructively and invasively growing cancer cells (36). Analysis of DNA microarray databases (www.oncomine.org) revealed a significant, tumor grade-dependent increase in fibronectin expression in NSCLC. Furthermore, patients dying within three years showed significantly higher fibronectin expression than patients still alive after three years, indicating that fibronectin expression may serve as a potential prognostic marker. Similar observations have been made in laryngeal, breast, and urothelial cancers (37–39). There is abundant, heterogenous ECM protein expression in tumors and their activated stroma. Radiotherapy (40) and, as shown here, molecular drugs like cetuximab induce ECM protein biosynthesis and remodeling – an event mostly neglected as a potential process of acquired resistance to therapy.

Published OnlineFirst August 15, 2013; DOI: 10.1158/0008-5472.CAN-13-0344

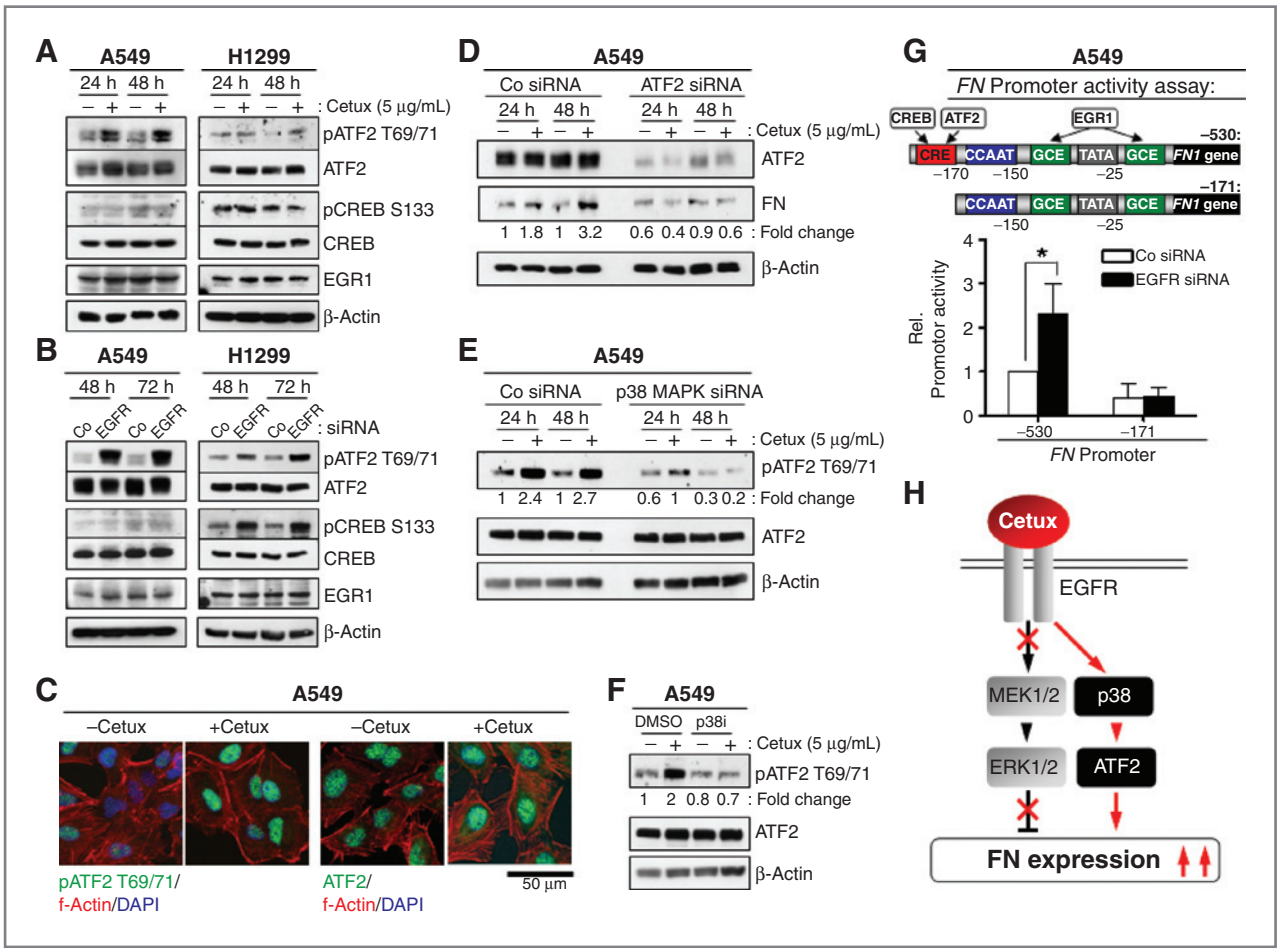

Figure 6. ATF2 mediates upregulation of fibronectin after EGFR inhibition. Western blot (A) of NSCLC cells treated with cetuximab (5 μg/mL) for 24 or 48 hours or after knockdown of EGFR (B). C, immunofluorescence staining of ATF2 and phosphorylated ATF2 in A549 cells 48 hours after treatment with cetuximab (5 μg/mL). D, after ATF2 siRNA transfection (nonspecific siRNA as control, Co), cells were treated with cetuximab for 24 or 48 hours and lysed for Western blot. Analysis of ATF2 expression and phosphorylation after p38 MAPK knockdown (nonspecific siRNA as control, Co; E) or exposure with p38 MAPK inhibitor (p38i; SB203680, 20 μmol/L; dimethyl sulfoxide as control; F). G, promoter activity of *FN* promoter constructs was measured by analyzing luciferase activity. A549 cells were transfected with EGFR siRNA or nonspecific siRNA (Co) for 48 hours. H, proposed mechanisms of how cetuximab inhibits the MEK/ERK pathway and, on the other side, activates p38 MAPK and ATF2, which results in increased fibronectin synthesis.

This strongly suggests that interactions of tumor cells with ECM proteins as well as therapy-induced ECM biosynthesis counteract modern multimodal cancer therapies. Confirmatory data for both issues are shown here as the tested A549 and H1299 human NSCLC cells show higher radioresistance as well as a diminished cytotoxic and radiosensitizing potential of cetuximab on adhesion to fibronectin. These findings corroborate published data in cells from other malignancies and on other drugs (41–43).

Intriguingly, fibronectin is apparently involved in how effectively EGFR inhibition mediates antisurvival biochemical cues. In normal cells, blocking EGFR signals leads to ECM production, cell differentiation, and anoikis in parallel to prevention of mitogenesis and migration (44, 45). It seems that these effects differentially occur in tumor cells dependent on EGFR mutations, tissue origin, and type of inhibitor (46), which challenges the rationale for patient selection for anti-EGFR agents. Moreover, these observations clearly reveal a tight spatiotemporal interaction between EGFR and cell-adhesion molecules like integrins. One might take advantage of adhesion-blocking compounds such as inhibitory anti-integrin antibodies to overcome resistance to anti-EGFR agents. Indeed, the effectiveness of anti-integrin compounds to reduced radio- and chemoresistance has been shown preclinically in head and neck and breast carcinoma models in combination with radio- or chemotherapy (32, 47).

Alternative approaches for preventing cetuximab autoinhibitory processes might target the signaling molecules involved in fibronectin biosynthesis and secretion. As cetuximab-inhibited EGFR stably remained in the cell membrane, p38 MAPK is a putative candidate differentially expressed in tumor versus normal tissues. Intriguingly, inhibition of protein kinases downstream of EGFR such as MEK1/2, ERK1/2, and PI3K led to increased fibronectin biosynthesis similar to that observed after EGFR blocking or downregulation. Targeting ATF2, whose contribution to the regulation of *FN1* gene expression

Published OnlineFirst August 15, 2013; DOI: 10.1158/0008-5472.CAN-13-0344

has been previously described (28), might cause severe side effects due its function as a transcription factor for a variety of other genes such as cyclin A and IFN-β (48). Mechanistically, ATF2, but not CREB or EGR1, is essential for fibronectin biosynthesis after EGFR blocking or knockdown in human NSCLC cells. Depletion of the −530 to −171 bp sequence of *FN1* gene promoter region, including the ATF2 binding site, completely abrogated the upregulation of *FN1* gene expression induced by depletion of EGFR.

In summary, antisurvival effects of the inhibitory anti-EGFR antibody cetuximab are counteracted by an autostimulation of specific resistance bypass signal transduction pathways. Evidently, extreme stimulation of ECM biosynthesis by cetuximab and adhesion to ECM proteins potently attenuate the cytotoxic and radiosensitizing potential of cetuximab. Deciphering in more detail the complex pathology of how EGFR mediates biochemical cues in cancer cells might be of particular importance for the optimization of individual patient selection for anti-EGFR strategies and the identification of novel approaches to prevent resistance mechanisms induced by anti-EGFR compounds themselves.

Disclosure of Potential Conflicts of Interest

No potential conflicts of interest were disclosed.

Authors' Contributions

Conception and design: I. Eke, N. Cordes
Development of methodology: I. Eke, N. Cordes
Acquisition of data (provided animals, acquired and managed patients, provided facilities, etc.): I. Eke, K. Storch, M. Krause
Analysis and interpretation of data (e.g., statistical analysis, biostatistics, computational analysis): I. Eke, K. Storch, N. Cordes
Writing, review, and/or revision of the manuscript: I. Eke, K. Storch, N. Cordes
Administrative, technical, or material support (i.e., reporting or organizing data, constructing databases): N. Cordes
Study supervision: N. Cordes

Acknowledgments

We thank S. Hehlgans, F. Schlegel, I. Lange and K. Schumann for excellent technical assistance.

Grant Support

The research and authors were, in part, financially supported by a grant from the Bundesministerium für Bildung und Forschung (BMBF Contracts 03ZIK041 and BMBF-02NUK006B to N. Cordes), the EFRE Europäische Fonds für regionale Entwicklung, Europa fördert Sachsen (100066308), and by a grant from the Medical Faculty (MeDDrive to I. Eke).

The costs of publication of this article were defrayed in part by the payment of page charges. This article must therefore be hereby marked *advertisement* in accordance with 18 U.S.C. Section 1734 solely to indicate this fact.

Received February 12, 2013; revised June 12, 2013; accepted July 13, 2013; published OnlineFirst August 15, 2013.

References

1. Mellinghoff IK, Sawyers CL. The emergence of resistance to targeted cancer therapeutics. Pharmacogenomics 2002;3:603–23.
2. Voltz E, Gronemeyer H. A new era of cancer therapy: cancer cell targeted therapies are coming of age. Int J Biochem Cell Biol 2008;40:1–8.
3. Hynes NE, MacDonald G. ErbB receptors and signaling pathways in cancer. Curr Opin Cell Biol 2009;21:177–84.
4. Patel R, Leung HY. Targeting the EGFR-family for therapy: biological challenges and clinical perspective. Curr Pharm Des 2012;18:2672–9.
5. Morgensztern D, Govindan R. Is there a role for cetuximab in non small cell lung cancer? Clin Cancer Res 2007;13:s4602–5.
6. Zips D, Krause M, Yaromina A, Dorfler A, Eicheler W, Schutze C, et al. Epidermal growth factor receptor inhibitors for radiotherapy: biological rationale and preclinical results. J Pharm Pharmacol 2008;60:1019–28.
7. Bonner JA, Harari PM, Giralt J, Azarnia N, Shin DM, Cohen RB, et al. Radiotherapy plus cetuximab for squamous-cell carcinoma of the head and neck. N Engl J Med 2006;354:567–78.
8. Bonner JA, Harari PM, Giralt J, Cohen RB, Jones CU, Sur RK, et al. Radiotherapy plus cetuximab for locoregionally advanced head and neck cancer: 5-year survival data from a phase 3 randomised trial, and relation between cetuximab-induced rash and survival. Lancet Oncol 2010;11:21–8.
9. Jonker DJ, O'Callaghan CJ, Karapetis CS, Zalcberg JR, Tu D, Au HJ, et al. Cetuximab for the treatment of colorectal cancer. N Engl J Med 2007;357:2040–8.
10. Ettinger DS. Emerging profile of cetuximab in non-small cell lung cancer. Lung Cancer 2009;68:332–7.
11. Hirsch FR, Herbst RS, Olsen C, Chansky K, Crowley J, Kelly K, et al. Increased EGFR gene copy number detected by fluorescent *in situ* hybridization predicts outcome in non-small-cell lung cancer patients treated with cetuximab and chemotherapy. J Clin Oncol 2008;26:3351–7.
12. Guha U, Chaerkady R, Marimuthu A, Patterson AS, Kashyap MK, Harsha HC, et al. Comparisons of tyrosine phosphorylated proteins in cells expressing lung cancer-specific alleles of EGFR and KRAS. Proc Natl Acad Sci U S A 2008;105:14112–7.
13. Mack PC, Holland WS, Redman M, Lara PN Jr, Snyder LJ, Hirsch FR, et al. KRAS mutation analysis in cetuximab-treated advanced stage non-small cell lung cancer (NSCLC): SWOG experience with S0342 and S0536. J Clin Oncol (Meeting Abstracts) 2009;27:8022.
14. Ohashi K, Sequist LV, Arcila ME, Moran T, Chmielecki J, Lin YL, et al. Lung cancers with acquired resistance to EGFR inhibitors occasionally harbor BRAF gene mutations but lack mutations in KRAS, NRAS, or MEK1. Proc Natl Acad Sci U S A 2012;109:E2127–33.
15. Ricono JM, Huang M, Barnes LA, Lau SK, Weis SM, Schlaepfer DD, et al. Specific cross-talk between epidermal growth factor receptor and integrin alphavbeta5 promotes carcinoma cell invasion and metastasis. Cancer Res 2009;69:1383–91.
16. Cabodi S, Morello V, Masi A, Cicchi R, Broggio C, Distefano P, et al. Convergence of integrins and EGF receptor signaling via PI3K/Akt/FoxO pathway in early gene Egr-1 expression. J Cell Physiol 2009;218:294–303.
17. Eke I, Schneider L, Forster C, Zips D, Kunz-Schughart LA, Cordes N. EGFR/JIP-4/JNK2 signaling attenuates cetuximab-mediated radiosensitization of squamous cell carcinoma cells. Cancer Res 2012;73:297–306.
18. Eke I, Sandfort V, Mischkus A, Baumann M, Cordes N. Antiproliferative effects of EGFR tyrosine kinase inhibition and radiation-induced genotoxic injury are attenuated by adhesion to fibronectin. Radiother Oncol 2006;80:178–84.
19. Eke I, Sandfort V, Storch K, Baumann M, Roper B, Cordes N. Pharmacological inhibition of EGFR tyrosine kinase affects ILK-mediated cellular radiosensitization *in vitro*. Int J Radiat Biol 2007;83:793–802.
20. Giannelli G, Azzariti A, Fransvea E, Porcelli L, Antonaci S, Paradiso A. Laminin-5 offsets the efficacy of gefitinib ('Iressa') in hepatocellular carcinoma cells. Br J Cancer 2004;91:1964–9.
21. Yarwood SJ, Woodgett JR. Extracellular matrix composition determines the transcriptional response to epidermal growth factor receptor activation. Proc Natl Acad Sci U S A 2001;98:4472–7.
22. Leiss M, Beckmann K, Giros A, Costell M, Fassler R. The role of integrin binding sites in fibronectin matrix assembly in vivo. Curr Opin Cell Biol 2008;20:502–7.

23. Wernert N. The multiple roles of tumour stroma. Virchows Arch 1997;430:433–43.
24. Labat-Robert J. Fibronectin in malignancy. Semin Cancer Biol 2002;12:187–95.
25. Bissell MJ, Kenny PA, Radisky DC. Microenvironmental regulators of tissue structure and function also regulate tumor induction and progression: the role of extracellular matrix and its degrading enzymes. Cold Spring Harb Symp Quant Biol 2005;70:343–56.
26. Kaspar M, Zardi L, Neri D. Fibronectin as target for tumor therapy. Int J Cancer 2006;118:1331–9.
27. Jerhammar F, Ceder R, Garvin S, Grenman R, Grafstrom RC, Roberg K. Fibronectin 1 is a potential biomarker for radioresistance in head and neck squamous cell carcinoma. Cancer Biol Ther 2010;10:1244–51.
28. Alonso CR, Pesce CG, Kornblihtt AR. The CCAAT-binding proteins CP1 and NF-I cooperate with ATF-2 in the transcription of the fibronectin gene. J Biol Chem 1996;271:22271–9.
29. Zayzafoon M, Botolin S, McCabe LR. P38 and activating transcription factor-2 involvement in osteoblast osmotic response to elevated extracellular glucose. J Biol Chem 2002;277:37212–8.
30. Liu C, Yao J, Mercola D, Adamson E. The transcription factor EGR-1 directly transactivates the fibronectin gene and enhances attachment of human glioblastoma cell line U251. J Biol Chem 2000;275:20315–23.
31. Tsuda M, Takahashi S, Takahashi Y, Asahara H. Transcriptional co-activators CREB-binding protein and p300 regulate chondrocyte-specific gene expression via association with Sox9. J Biol Chem 2003;278:27224–9.
32. Eke I, Deuse Y, Hehlgans S, Gurtner K, Krause M, Baumann M, et al. beta (1)Integrin/FAK/cortactin signaling is essential for human head and neck cancer resistance to radiotherapy. J Clin Invest 2012;122:1529–40.
33. Eke I, Koch U, Hehlgans S, Sandfort V, Stanchi F, Zips D, et al. PINCH1 regulates Akt1 activation and enhances radioresistance by inhibiting PP1alpha. J Clin Invest 2010;120:2516–27.
34. Gurtner K, Deuse Y, Butof R, Schaal K, Eicheler W, Oertel R, et al. Diverse effects of combined radiotherapy and EGFR inhibition with antibodies or TK inhibitors on local tumour control and correlation with EGFR gene expression. Radiother Oncol 2011;99:323–30.
35. Eke I, Leonhardt F, Storch K, Hehlgans S, Cordes N. The small molecule inhibitor QLT0267 radiosensitizes squamous cell carcinoma cells of the head and neck. PLoS One 2009;4:e6434.
36. Lu P, Takai K, Weaver VM, Werb Z. Extracellular matrix degradation and remodeling in development and disease. Cold Spring Harb Perspect Biol 2011;3;pii-a005058.
37. Pietruszewska W, Kobos J, Bojanowska-Pozniak K, Durko M, Gryczynski M. Immunohistochemical analysis of the fibronectin expression and its prognostic value in patients with laryngeal cancer. Otolaryngol Pol 2006;60:697–702.
38. Ioachim E, Charchanti A, Briasoulis E, Karavasilis V, Tsanou H, Arvanitis DL, et al. Immunohistochemical expression of extracellular matrix components tenascin, fibronectin, collagen type IV and laminin in breast cancer: their prognostic value and role in tumour invasion and progression. Eur J Cancer 2002;38:2362–70.
39. Ioachim E, Michael M, Stavropoulos NE, Kitsiou E, Salmas M, Malamou-Mitsi V. A clinicopathological study of the expression of extracellular matrix components in urothelial carcinoma. BJU Int 2005;95:655–9.
40. Rintoul RC, Sethi T. The role of extracellular matrix in small-cell lung cancer. Lancet Oncol 2001;2:437–42.
41. Stevenson AF, Lange CS. Extracellular matrix (ECM) and cytoskeletal modulation of cellular radiosensitivity. Acta Oncol 1997;36:599–606.
42. Cordes N, Meineke V. Cell adhesion-mediated radioresistance (CAM-RR). Extracellular matrix-dependent improvement of cell survival in human tumor and normal cells in vitro. Strahlenther Onkol 2003;179:337–44.
43. Aoudjit F, Vuori K. Integrin signaling in cancer cell survival and chemoresistance. Chemother Res Pract 2012;2012:283181.
44. Reginato MJ, Mills KR, Paulus JK, Lynch DK, Sgroi DC, Debnath J, et al. Integrins and EGFR coordinately regulate the pro-apoptotic protein Bim to prevent anoikis. Nat Cell Biol 2003;5:733–40.
45. Bill HM, Knudsen B, Moores SL, Muthuswamy SK, Rao VR, Brugge JS, et al. Epidermal growth factor receptor-dependent regulation of integrin-mediated signaling and cell cycle entry in epithelial cells. Mol Cell Biol 2004;24:8586–99.
46. Barkovich KJ, Hariono S, Garske AL, Zhang J, Blair JA, Fan QW, et al. Kinetics of inhibitor cycling underlie therapeutic disparities between EGFR-driven lung and brain cancers. Cancer Discov 2012;2:450–7.
47. Nam JM, Onodera Y, Bissell MJ, Park CC. Breast cancer cells in three-dimensional culture display an enhanced radioresponse after coordinate targeting of integrin alpha5beta1 and fibronectin. Cancer Res 2010;70:5238–48.
48. Bhoumik A, Fichtman B, Derossi C, Breitwieser W, Kluger HM, Davis S, et al. Suppressor role of activating transcription factor 2 (ATF2) in skin cancer. Proc Natl Acad Sci U S A 2008;105:1674–9.

Cancer Research
The Journal of Cancer Research (1916–1930) | The American Journal of Cancer (1931–1940)

AACR American Association for Cancer Research

Cetuximab Attenuates Its Cytotoxic and Radiosensitizing Potential by Inducing Fibronectin Biosynthesis

Iris Eke, Katja Storch, Mechthild Krause, et al.

Cancer Res Published OnlineFirst August 15, 2013.